AMERICAN SOCIETY FOR MICROBIOLOGY | Journal of Bacteriology

Bacteriology | Full-Length Text

PmrAB, the two-component system of *Acinetobacter baumannii*, controls the phosphoethanolamine modification of lipooligosaccharide in response to metal ions

Noriteru Yamada,[1,2] Go Kamoshida,[1,3] Tsukasa Shiraishi,[4] Daiki Yamaguchi,[1] Momoko Matsuoka,[1] Reika Yamauchi,[1] Nana Kanda,[1] Roku Kamioka,[1] Norihiko Takemoto,[5] Yuji Morita,[3] Masahiro Fujimuro,[2] Shin-ichi Yokota,[4] Kinnosuke Yahiro[1]

AUTHOR AFFILIATIONS See affiliation list on p. 16.

ABSTRACT *Acinetobacter baumannii* is highly resistant to antimicrobial agents, and XDR strains have become widespread. *A. baumannii* has developed resistance to colistin, which is considered the last resort against XDR Gram-negative bacteria, mainly caused by lipooligosaccharide (LOS) phosphoethanolamine (pEtN) and/or galactosamine (GalN) modifications induced by mutations that activate the two-component system (TCS) *pmrAB*. Although PmrAB of *A. baumannii* has been recognized as a drug resistance factor, its function as TCS, including its regulatory genes and response factors, has not been fully elucidated. In this study, to clarify the function of PmrAB as TCS, we elucidated the regulatory genes (regulon) of PmrAB via transcriptome analysis using *pmrAB*-activated mutant strains. We discovered that PmrAB responds to low pH, Fe^{2+}, Zn^{2+}, and Al^{3+}. *A. baumannii* selectively recognizes Fe^{2+} rather than Fe^{3+}, and a novel region ExxxE, in addition to the ExxE motif sequence, is involved in the environmental response. Furthermore, PmrAB participates in the phosphoethanolamine modification of LOS on the bacterial surface in response to metal ions such as Al^{3+}, contributing to the attenuation of Al^{3+} toxicity and development of resistance to colistin and polymyxin B in *A. baumannii*. This study demonstrates that PmrAB in *A. baumannii* not only regulates genes that play an important role in drug resistance but is also involved in responses to environmental stimuli such as metal ions and pH, and this stimulation induces LOS modification. This study reveals the importance of PmrAB in the environmental adaptation and antibacterial resistance emergence mechanisms of *A. baumannii*.

IMPORTANCE Antimicrobial resistance (AMR) is a pressing global issue in human health. *Acinetobacter baumannii* is notably high on the World Health Organization's list of bacteria for which new antimicrobial agents are urgently needed. Colistin is one of the last-resort drugs used against extensively drug-resistant (XDR) Gram-negative bacteria. However, *A. baumannii* has become increasingly resistant to colistin, primarily by modifying its lipooligosaccharide (LOS) via activating mutations in the two-component system (TCS) PmrAB. This study comprehensively elucidates the detailed mechanism of drug resistance of PmrAB in *A. baumannii* as well as its biological functions. Understanding the molecular biology of these molecules, which serve as drug resistance factors and are involved in environmental recognition mechanisms in bacteria, is crucial for developing fundamental solutions to the AMR problem.

KEYWORDS *Acinetobacter baumannii*, PmrAB, lipopolysaccharide, colistin, LPS modification

Although antimicrobial agents have been used to treat *Acinetobacter baumannii* (a common Gram-negative bacterium) infections occurring in medical facilities,

Editor Michael Y. Galperin, NCBI, NLM, National Institutes of Health, Bethesda, Maryland, USA

Address correspondence to Go Kamoshida, kamoshida@my-pharm.ac.jp.

The authors declare no conflict of interest.

See the funding table on p. 16.

Received 18 December 2023
Accepted 3 April 2024
Published 25 April 2024

particularly in intensive care units (1–6), the prevalence of XDR *A. baumannii* strains has been increasing, limiting effective treatment options (7). Although broad-spectrum carbapenems are widely used to treat such infections (8), the prevalence of carbapenem-resistant *A. baumannii* (9) required a shift in therapeutic strategies (10).

Colistin, a cationic polypeptide antimicrobial agent, is critical in treating XDR *A. baumannii* infections, including those resistant to carbapenems (11, 12). Colistin binds to lipopolysaccharide (LPS) on the outer membrane of Gram-negative bacteria, destabilizing the cell membrane and leading to bactericidal activity (13). As the LPS in *A. baumannii* lacks O antigen and is instead characterized as LOS, the emergence of colistin-resistant *A. baumannii* strains has been reported, complicating treatment against these strains (11–15). The primary mechanism of colistin resistance in *A. baumannii* involves mutations in the two-component *pmrAB* gene system (16), which increase LOS modifications (phosphoethanolamine [pEtN] via *pmrC* and galactosamine [GalN] via *naxD*) and decrease colistin binding (17–20). However, the LOS modification that is crucial for colistin resistance is unclear.

PmrAB regulates the expression of specific genes (regulons) by activating (phosphorylating) the response regulator PmrA in response to environmental factors (21). A PmrAB regulon in *Salmonella* has been identified (22), with PmrB in *Salmonella* responding to extracellular environmental factors such as Fe^{3+}, Al^{3+}, and low pH (23–27), suggesting that PmrB responds to metal ions and pH changes. *A. baumannii* responds to low pH but does not respond to metal ions such as Fe^{3+} (28, 29). The environmental factors that PmrAB of *A. baumannii* responds to, excluding pH, are poorly understood. Moreover, the PmrAB regulon in *A. baumannii* has not been fully identified. Thus, PmrAB establishes drug resistance and regulates the specific regulons in response to unknown environmental factors but its biological mechanism remains undetermined. This study aimed to elucidate the molecular biology of the PmrAB regulon and its activators in *A. baumannii* to understand the role of PmrAB in *A. baumannii* response to environmental factors.

RESULTS

Elucidation of the PmrAB regulon in *A. baumannii*

Previous research on the *A. baumannii* PmrAB system has predominantly utilized *pmrAB* mutant clinical isolates to deduce its regulon (30–32). However, this approach is limited by the lack of whole-genome sequences and the varying genetic backgrounds of different strains. A library of *pmrAB*-activating mutants with identical genetic backgrounds of *A. baumannii* has been successfully established using specific drug selection on the standard strain ATCC 19606 and the drug-resistant clinical isolate ATCC BAA-1605 (33). This library was utilized to select representative mutants for both *pmrA* and *pmrB* that were previously reported in clinical strains (PmrA: M12I, PmrB: P233S) (34–36) and those not reported (PmrA: I13S, PmrB: R263G). In addition to these four strains (Fig. S1), an artificial disruption of the *pmrA* gene was created in a *pmrB*-activating mutant strain (Δ*pmrA*-CM012S), thus forming a set of five representative strains in total. For ATCC BAA-1605, one representative strain was chosen from each *pmrA*- and *B*-activating mutant (PmrA: L20F and PmrB: P233S). Whole-genome analysis confirmed that these strains harbored no mutations other than those in *pmrA* and *B*. RNA-seq analysis of these strains identified 18 genes upregulated in the *pmrAB* mutant strain derived from ATCC 19606 strain, including those involved in autoregulation of the *pmrCAB* operon, and in addition to other LOS modification genes (*eptA*: pEtN modification gene and *naxD*), in the biosynthesis of polysaccharide poly-β-1,6-N-acetyl-D-glucosamine (*pgaB*, *C*, *D*; Fig. 1). All genes upregulated in the ATCC 19606 strain were found to be upregulated in the ATCC BAA-1605 *pmrAB* mutant strains as well, except for *eptA* that was not on the chromosome, thus resulting in 17 upregulated genes. Additional genes, including *csuAB* and three unknown genes, were upregulated in ATCC BAA-1605 (Fig. S2).

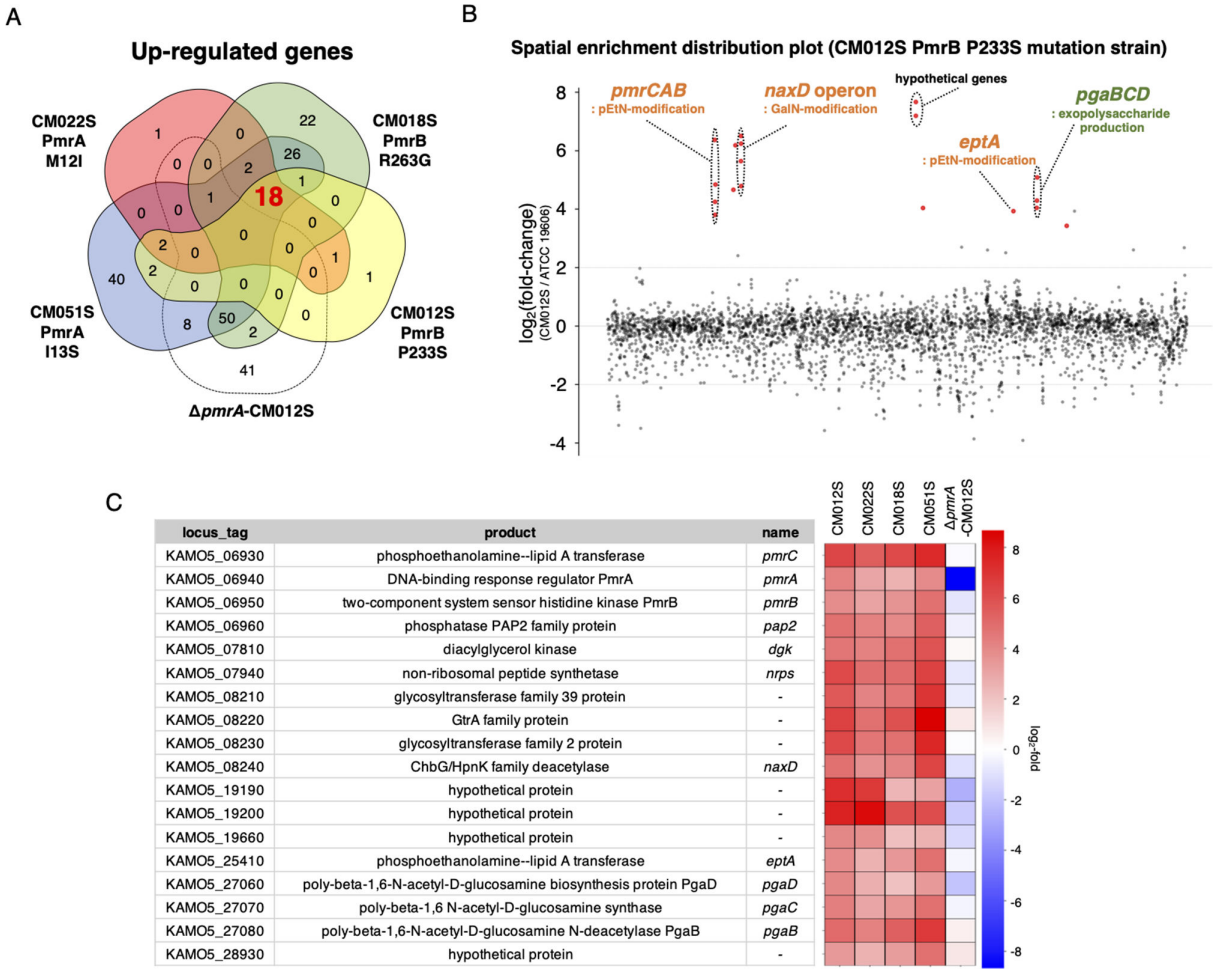

locus_tag	product	name
KAMO5_06930	phosphoethanolamine--lipid A transferase	*pmrC*
KAMO5_06940	DNA-binding response regulator PmrA	*pmrA*
KAMO5_06950	two-component system sensor histidine kinase PmrB	*pmrB*
KAMO5_06960	phosphatase PAP2 family protein	*pap2*
KAMO5_07810	diacylglycerol kinase	*dgk*
KAMO5_07940	non-ribosomal peptide synthetase	*nrps*
KAMO5_08210	glycosyltransferase family 39 protein	-
KAMO5_08220	GtrA family protein	-
KAMO5_08230	glycosyltransferase family 2 protein	-
KAMO5_08240	ChbG/HpnK family deacetylase	*naxD*
KAMO5_19190	hypothetical protein	-
KAMO5_19200	hypothetical protein	-
KAMO5_19660	hypothetical protein	-
KAMO5_25410	phosphoethanolamine--lipid A transferase	*eptA*
KAMO5_27060	poly-beta-1,6-N-acetyl-D-glucosamine biosynthesis protein PgaD	*pgaD*
KAMO5_27070	poly-beta-1,6 N-acetyl-D-glucosamine synthase	*pgaC*
KAMO5_27080	poly-beta-1,6-N-acetyl-D-glucosamine N-deacetylase PgaB	*pgaB*
KAMO5_28930	hypothetical protein	-

FIG 1 Elucidation of the PmrAB regulon in *A. baumannii* by RNA-seq. (A) Genes with $\log_2$ (fold change) ≥ 2 and *P* value < 0.05 compared with the WT strain were considered significantly upregulated, and Venn diagrams were generated to illustrate this. The 18 genes common to the *pmrA* and *B* mutants but not to Δ*pmrA*-CM012S were identified as regulons. (B) A spatial enrichment distribution plot of CM012S (*pmrB*-activating mutant strain) is presented. The vertical axis indicates $\log_2$ (fold change), and the horizontal axis represents gene loci in the genome sequence. Red dots indicate regulon genes (18 genes). (C) List of the upregulated 18 regulon genes in the ATCC 19606 *pmrAB*-activating mutant strain is provided, which shows the locus tag of the ATCC 19606 strain (GenBank accession number: AP025740.1), its product, gene name, and expression levels of each gene in each strain, depicted on a heatmap.

Construction of a PmrAB reporter assay system for *A. baumannii*

To elucidate the response of PmrAB in *A. baumannii*, we developed a reporter assay system using β-galactosidase activity. We identified KAMO5_07940, a gene locus encoding a non-ribosomal peptide synthase (NRPS), whose expression is significantly upregulated by PmrAB [*P* value = 2.20×10^{-178}, $\log_2$ (fold change) = 6.18 in CM012S; Fig. 2A]. Analysis of the 200-bp upstream regions of the 18 upregulated genes using MEME Suite (37) revealed a DNA consensus sequence (-TTTAAN$_6$TTTAA-) upstream of all genes (except those forming operons; Fig. 2B). This motif is also present upstream of the NRPS gene. Based on these findings, we constructed a reporter plasmid that utilizes the upstream region of the NRPS gene to precisely evaluate PmrAB activity (Fig. 2C). When the reporter plasmid was introduced into PmrAB-active mutant strains (CM022S PmrA M12I and CM012S PmrB P233S), the β-galactosidase activity drastically increased. This effect was not observed for the PmrA knockout strain (Δ*pmrA*-CM012S; Fig. 2D). This result confirmed the establishment of the reporter assay system for evaluating PmrAB activation in *A. baumannii*.

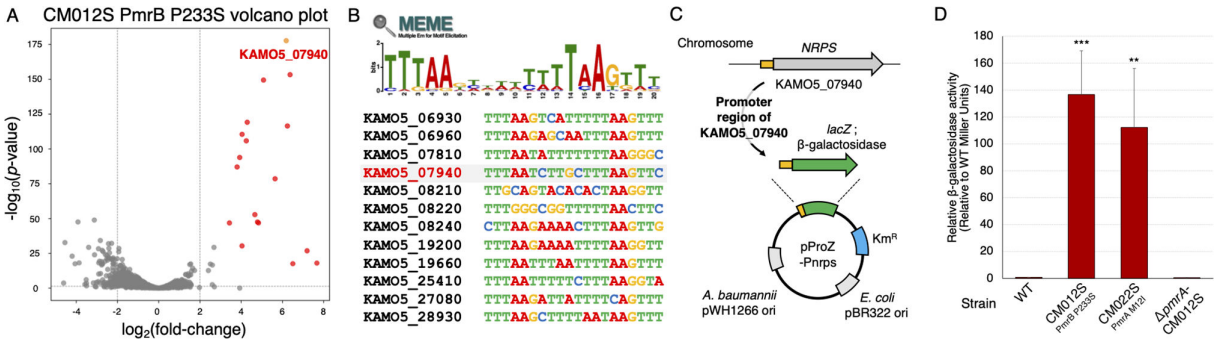

FIG 2 Construction of the PmrAB reporter assay system for *A. baumannii*. RNA-seq analysis was conducted on the *pmrB*-activating mutant strain CM012S (P233S mutant), established from ATCC 19606 (WT strain). (A) A volcano plot comparing the CM012S strain with the WT strain is presented. The red dots (representing 17 genes) signify the PmrAB regulon. The gene KAMO5_07940, which is significantly upregulated [*P* value = 2.20×10^{-178}, $\log_2$ (fold change) = 6.18], is highlighted with a yellow dot. (B) The 200-bp upstream region of the PmrAB regulon genes was extracted, and a consensus sequence predicted to bind PmrA was identified using the MEME Suite. (C) A schematic diagram of the reporter plasmid pProZ-Pnrps. Based on shuttle vectors for *A. baumannii* and *E. coli*, the *lacZ* gene encoding β-galactosidase was introduced downstream of the promoter region upstream of the KAMO5_07940 gene. (D) The pProZ-Pnrps plasmid was introduced into CM012S (*pmrB* mutation strain), CM022S (*pmrA* mutation strain), and *pmrA* disruption in *pmrB*-activating strain (*pmrA*-CM012S), and relative β-galactosidase activity was measured. Experiments were conducted independently in triplicate, and the results are presented as mean values with standard deviations represented by error bars. Statistical significance is shown as a reference of the WT strain mRNA levels using Dunnett's test; ***$P < 0.001$, **$P < 0.01$.

A. baumannii PmrAB responds to Fe^{2+}, Zn^{2+}, and Al^{3+}

The wild-type (WT) ATCC 19606 strain and the Δ*pmrA* and Δ*pmrB* strains were transformed with the reporter plasmid. These strains were exposed to low pH (pH 5.8) and to 500 µM each of the various indicated metal ions, following which the β-galactosidase activity was measured (Fig. 3A). We detected high β-galactosidase activity at low pH (Fig. 3B). Furthermore, we discovered that PmrAB of *A. baumannii* responds to metal ions such as Fe^{2+}, Zn^{2+}, and Al^{3+} (Fig. 3C). The mRNA expression level of autoregulated *pmrCAB* increased in response to Fe^{2+}, Zn^{2+}, and Al^{3+} (Fig. S3A). A similar trend was observed for pH induction, although the difference was not statistically significant (Fig. S3B). Another strain of *A. baumannii*, ATCC 17978, similarly responded to pH 5.8, Fe^{2+}, Zn^{2+}, and Al^{3+} (Fig. S3C and S3D).

Notably, PmrAB of *A. baumannii* did not respond to Fe^{3+}, suggesting selective responsiveness to Fe^{2+}. Next, we examined whether PmrAB discriminates between Fe^{2+} and Fe^{3+}. The activity of β-galactosidase increased in a concentration-dependent manner in response to Fe^{2+} treatment but was comparatively low for Fe^{3+} (Fig. 3D). Furthermore, when we employed sodium ascorbate as a reducing agent to reduce Fe^{3+} to Fe^{2+} (38), β-galactosidase activity increased in a concentration-dependent manner (Fig. 3E). These results suggest that PmrAB of *A. baumannii* TCS selectively recognizes Fe^{2+} rather than Fe^{3+}.

PmrB 35-ExxE-38 and 131-ExxxE-135 motifs in the periplasmic region are essential for response to low pH and metal ions in *A. baumannii*

In other species of PmrAB, the ExxE motif sequence in the periplasmic region of PmrB is essential for response to metal ions and low pH (25, 27). In *A. baumannii* PmrB, one ExxE (35-EVDE-38) motif was identified in the periplasmic region as predicted by TMHMM (39). Additionally, two ExxxE motifs (49-ERTAE-53 and 131-ERVRE-135), each with an extra-amino acid between the glutamate residues, were found in the periplasmic region (Fig. 4A). To determine which motifs are critical for the environmental response of *A. baumannii* PmrB, we generated mutants in which the glutamate in the ExxE/ExxxE motifs was replaced by alanine and conducted a reporter assay. These mutant strains were exposed to low pH, Fe^{2+}, Zn^{2+}, or Al^{3+}, following which the activity of β-galactosidase was compared with that of the wild-type strain (PmrB WT). The 35-ExxE-38 motif was important for stimulation by low pH, Fe^{2+}, Zn^{2+}, or Al^{3+}, as expected (Fig. 4B and C). Notably, the

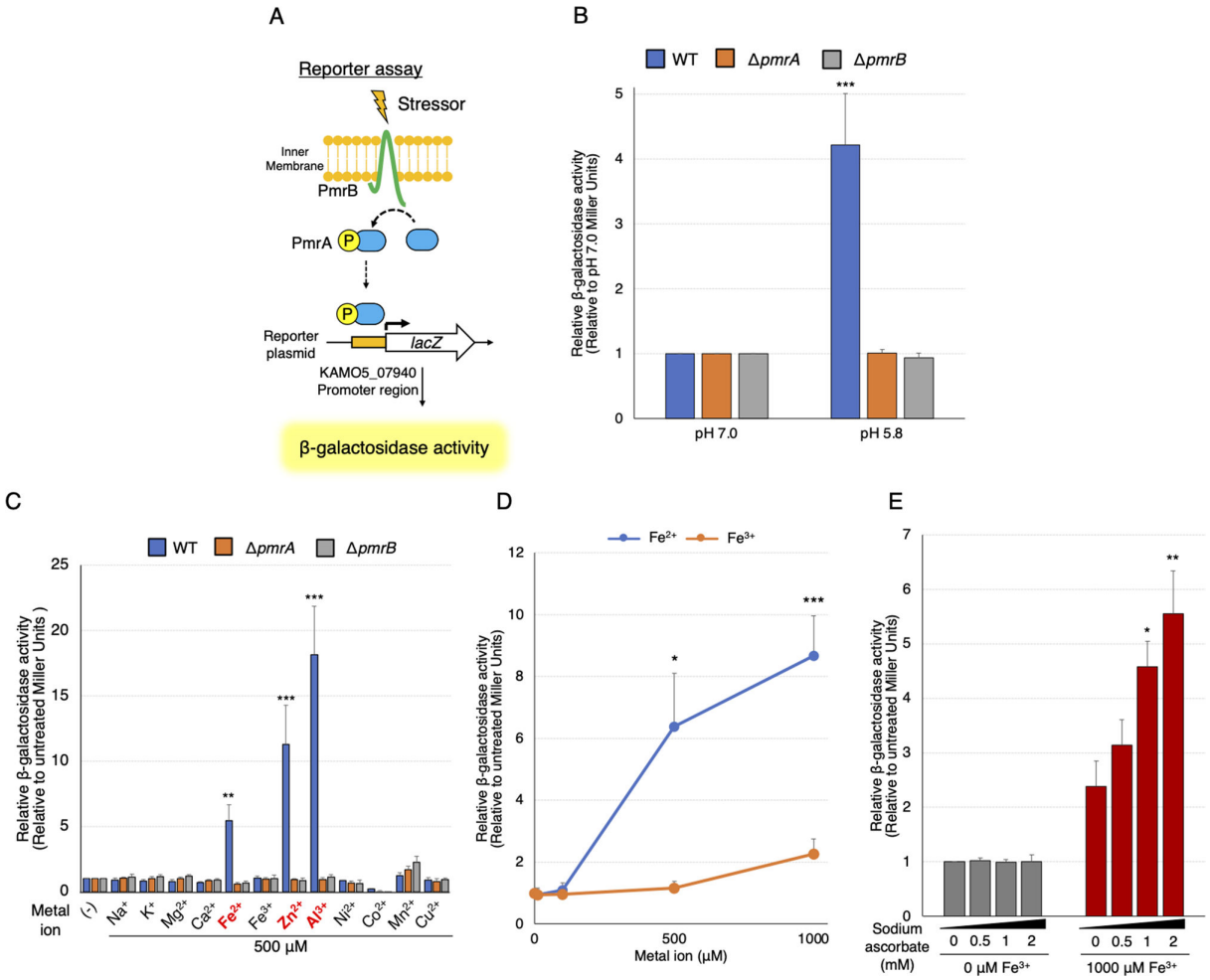

FIG 3 Identification of PmrAB response factors in *A. baumannii*. (A) A schematic diagram of the PmrAB reporter assay in *A. baumannii*. Upon activation of PmrB, PmrA is phosphorylated and binds to the upstream region of the KAMO5_07940 gene, which induces *lacZ* expression and produces β-galactosidase. The β-galactosidase activity was evaluated after incubation at pH 7.0 or 5.8 (B) or with 500 µM NaCl, KCl, $MgCl_2$, $CaCl_2$, $FeSO_4$, $FeCl_3$, $ZnSO_4$, $AlCl_3$, $NiSO_4$, $Co(NO_3)_2$, $MnCl_2$, or $CuSO_4$ (C) for 60 min. The values are expressed as relative values, with those at pH 7.0 or without metal ions set at 1.0. (D) Relative β-galactosidase activity is shown after 60 min of incubation with Fe^{2+} ($FeSO_4$) or Fe^{3+} ($FeCl_3$) at concentrations of 0, 100, 500, or 1,000 µM for the ATCC 19606 strain harboring the reporter plasmid. (E) β-galactosidase activity was evaluated after 60 min of incubation of the ATCC 19606 strain transfected with the reporter plasmid with or without 1,000 µM of $FeCl_3$, and with 0, 0.5, 1, or 2 mM of ascorbic acid used as a reducing agent. The values are shown as relative values, with the value without $FeCl_3$ addition set at 1.0. All experiments were performed in triplicate. Mean values and error bars represent standard deviations. Statistical significance is shown using Tukey's test as a reference of pH 7.0 or untreated values (B, C), unpaired *t*-test compares Fe^{2+} and Fe^{3+} (D), and Dunnett's test as a reference of the untreated value (E); ***$P < 0.001$, **$P < 0.01$, *$P < 0.05$.

strain with alanine substituted for glutamate at 131-ExxxE-135 (strain 131-AxxxA-135) exhibited a considerably reduced response to low pH (Fig. 4B). Conversely, in the strain 131-AxxxA-135, responsiveness to Fe^{2+} and Al^{3+} did not change; however, responsiveness to Zn^{2+} was reduced to approximately 60% of that of the parent strain (Fig. 4C). Furthermore, the results showed that strain 131-AxxxA-135 stimulated by Zn^{2+} showed reduced resistance to polymyxin B, which was less responsive compared to the WT strain (Fig. 4D; Fig. S4). Hence, we found a functional motif 131-ExxxE-135 of PmrB. Moreover, the 49-ExxxE-53 motif had little effect on these environmental responses. These findings suggest that the 35-ExxE-38 and 131-ExxxE-135 motifs are the major amino acid sequences involved in the response to metal ions and low pH in PmrB.

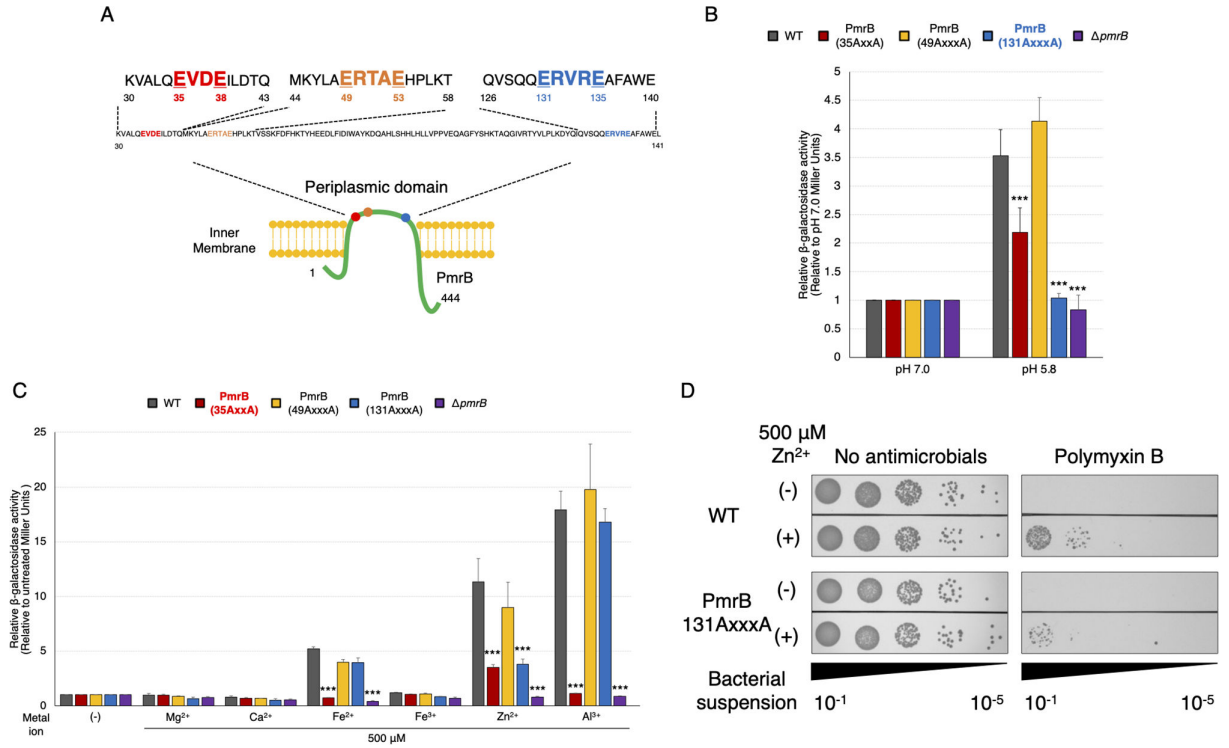

FIG 4 Altered responsiveness of *A. baumannii* PmrB motif sequence mutants to low pH and metal ions. (A) A schematic diagram of the amino acid sequence in the PmrB periplasmic region of *A. baumannii* is presented. Mutant strains with alanine substitutions for glutamate in the ExxE and ExxxE motifs were generated and transfected with a reporter plasmid. These were then incubated at pH 7.0 or 5.8 (B), and β-galactosidase activity was measured after incubation with 500 µM NaCl, KCl, $MgCl_2$, $CaCl_2$, $FeSO_4$, $FeCl_3$, $ZnSO_4$, $AlCl_3$, $NiSO_4$, $Co(NO_3)_2$, $MnCl_2$, or $CuSO_4$ for 60 min (C). The values are presented as relative values, with those at pH 7.0 or without metal ions set at 1.0. All experiments were performed in triplicate. Mean values and error bars represent standard deviations. Statistical significance is shown as a reference of the ATCC 19606 (WT) strain value using Dunnett's test; ***$P < 0.001$. (D) The WT and PmrB (131AxxxA) strains in the logarithmic growth phase were exposed to 500 µM $ZnSO_4$ for 2 h. Subsequently, the bacterial suspension was adjusted to an OD_{600} of 0.2. After incubating the bacterial suspension with 7 µg/mL polymyxin B or without antimicrobial agents for 2 h, 10 µL of the 10-fold serial dilution of the bacterial suspension was plated onto LB agar plates, which were then incubated at 37°C for 24 h. Experiments were conducted in triplicate, and images of representative agar plates are shown.

Mechanism of PmrAB-dependent lipid A modification and Al^{3+} toxicity avoidance in *A. baumannii*

Among the environmental factors, the most significant response, as detected by β-galactosidase activity for PmrAB, was elicited by Al^{3+}; therefore, we evaluated whether PmrAB induces phenotypic changes in response to Al^{3+}, including tolerance to colistin and polymyxin B, and lipid A modification. Stimulation by Al^{3+} induced resistance to colistin and polymyxin B in WT but not in the Δ*pmrA* and Δ*pmrB* strains (Fig. 5A). Next, we investigated the Al^{3+}-induced LOS modification using matrix-assisted laser desorption/ionization time-of-flight mass spectrometry (MALDI-TOF/MS). Al^{3+}-stimulated lipid A exhibited a peak at *m/z* 2033, indicating phosphoethanolamine (pEtN) modification (Fig. 5B; Fig. S5). The lipid A modification peak was absent in the Δ*pmrB* strain. Furthermore, the minimum inhibitory concentrations (MICs) of colistin were assessed both in the presence and absence of Al^{3+} (Table 1). The results showed that the addition of 500 µM Al^{3+} led to an increase in MICs for both the WT and the Δ*naxD* strain with a disrupted GalN modification gene. In contrast, the Δ*eptA* strain, associated with the pEtN modification, exhibited only a minor increase in colistin resistance. Notably, the Δ*pmrC*, Δ*pmrC*Δ*eptA*, and Δ*pmrC*Δ*eptA*Δ*naxD* strains did not show any increase in colistin resistance. These results indicated that PmrAB is activated by Al^{3+} stimulation, which results in phenotypic changes.

Treatment with excess Al^{3+} causes cytotoxicity in bacteria (40). Wild-type or PmrB-active strains (WT and CM012S) of *A. baumannii* also showed growth inhibition in an

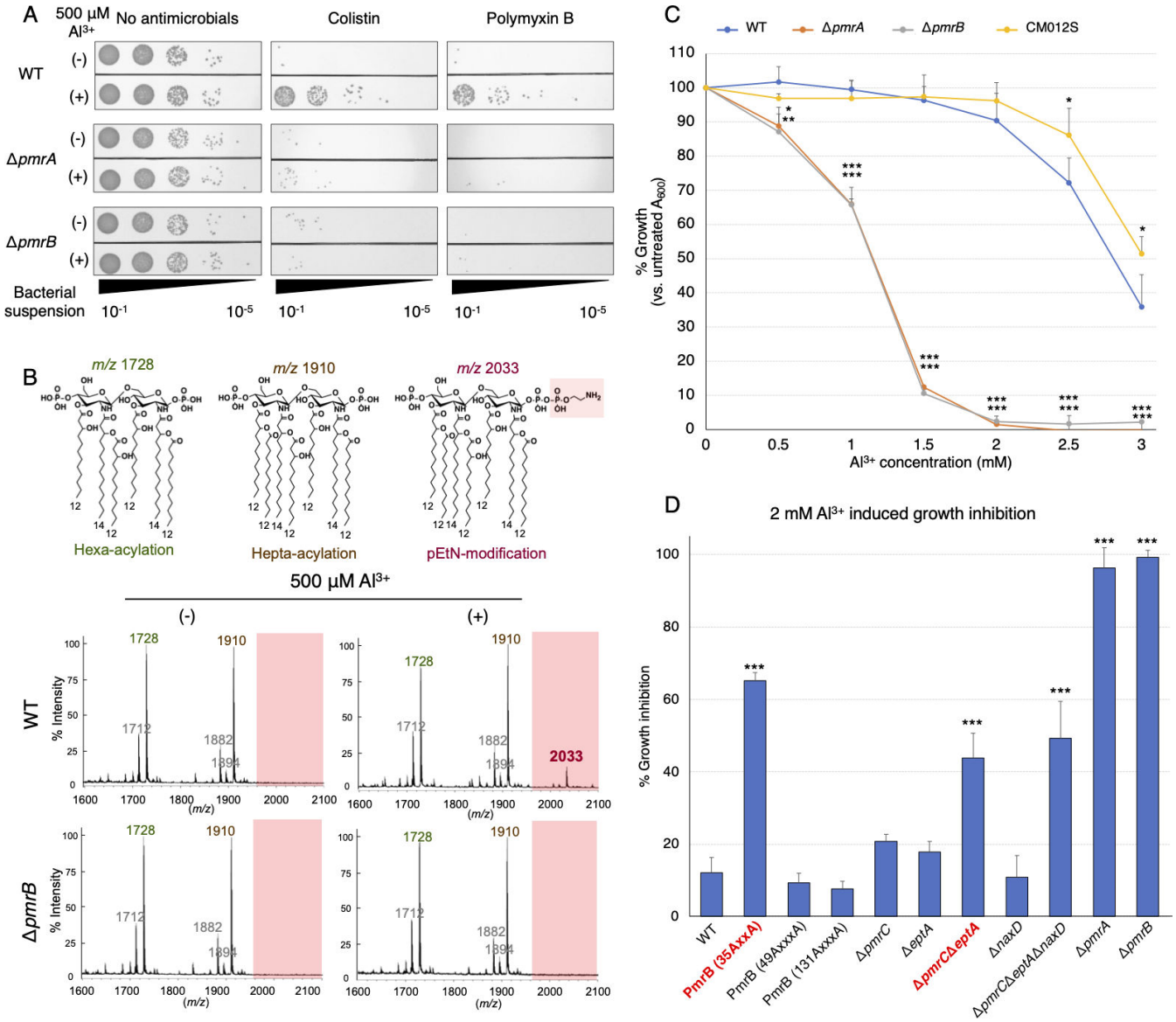

FIG 5 *A. baumannii* PmrAB-dependent phenotypic changes induced by Al^{3+}. (A) The ATCC 19606, Δ*pmrA*, and Δ*pmrB* strains in the logarithmic growth phase were exposed to 500 µM $AlCl_3$ for 2 h. Subsequently, the bacterial suspension was adjusted to an OD_{600} of 0.2. After incubating the bacterial suspension with 10 µg/mL colistin or 7 µg/mL polymyxin B, or without any antimicrobial agent (control) for 2 h, 10 µL of a 10-fold serial dilution (ranging from 10^{-1} to 10^{-5}) of the bacterial suspension was plated onto LB agar plates, which were then incubated at 37°C for 24 h. Experiments were conducted in triplicate, and images of representative agar plates are shown. (B)The ATCC 19606 (WT; middle row) and Δ*pmrB* strain (bottom row) in the logarithmic growth phase were exposed to 500 µM $AlCl_3$ for 2 h. Lipid A was extracted from the bacteria, and MALDI-TOF/MS was used to analyze its structure. The predicted structure of lipid A and its mass-to-charge ratio peaks are shown at the top. (C) The WT, Δ*pmrA*, Δ*pmrB*, and CM012S (PmrB P233S-activated mutant strain) strains were prepared at an OD_{600} of 0.001 and were incubated with the various indicated concentrations of $AlCl_3$ for 24 h. Absorbance A_{600} was monitored, and growth ability was expressed as a relative value, with the value without $AlCl_3$ addition set at 100%. (D) PmrB motif mutant strains (ExxE/ExxxE alanine substitution strain) and various LOS modification gene disruption strains (Δ*pmrC*Δ*eptA*, Δ*naxD*, Δ*pmrC*Δ*eptA*Δ*naxD*) were grown in LB broth containing 2 mM $AlCl_3$ for 24 h. A_{600} of the bacteria was measured, and the relative growth inhibition was calculated by subtracting the value from 100%. All experiments were performed in triplicate. Mean values and error bars represent standard deviations. Statistical significance is shown as a reference of the WT strain value using Dunnett's test; ***$P < 0.001$, **$P < 0.01$, *$P < 0.05$.

Al^{3+}-dose-dependent manner; however, this inhibition effect was more pronounced for the PmrAB-knockout strains (Fig. 5C). Modification of LPS is crucial for avoiding metal toxicity via PmrAB activation in *Salmonella* spp. and *Escherichia coli* (27, 41, 42). We investigated the capacity of PmrAB to reduce the cytotoxicity caused by excessive Al^{3+}

TABLE 1 Colistin MIC of various mutant strains in the presence of Al^{3+}

Colistin (μg/mL)	WT	Δ*pmrA*	Δ*pmrB*	Δ*pmrC*	Δ*eptA*	Δ*naxD*	Δ*pmrC* Δ*eptA*	Δ*pmrC* Δ*eptA* Δ*naxD*
0 μM Al^{3+}	2	2	2	2	2	2	2	2
500 μM Al^{3+}	8	2	2	2	4	8	2	2

by employing an altered metal ion-responsive strain with alanine substitutions in the ExxE/ExxxE motif and a strain deficient in the pEtN and/or GalN modification genes, both of which are regulated by PmrAB. The PmrB 35-AxxA-38 strain, which is not responsive to metal ions, exhibited decreased growth under excess Al^{3+}. Furthermore, disruption of the pEtN modification genes (Δ*pmrC*Δ*eptA*) also led to significant growth inhibition (Fig. 5D). Conversely, the extent of growth inhibition in the strain with only the disruption of Δ*pmrC*, Δ*eptA*, and the GalN modification gene (Δ*naxD*) was similar to that observed for the WT strain. These results suggested that PmrB senses excess Al^{3+} and modifies pEtN in LOS to reduce its toxicity.

Phosphoethanolamine modification of lipid A is more important than galactosamine modification for colistin and polymyxin B resistance in *A. baumannii*

As described in the previous section, Al^{3+} stimulation of WT strain resulted in the appearance of a pEtN-modified peak at *m/z* 2033. In *Salmonella* spp., changes in surface charge due to LPS modification are crucial for avoiding metal toxicity and for polymyxin B resistance following PmrAB activation (24). Therefore, we investigated which among the two—pEtN or GalN—modifications of LOS is more crucial for colistin and polymyxin B resistance in PmrAB-active mutants of *A. baumannii*. Finally, we generated strains with various disrupted LOS modification-related genes from the colistin-resistant *pmrB*-activating mutant strain CM012S (Fig. S6A). We evaluated their survival on Luria-Bertani (LB) agar containing colistin and polymyxin B, and analyzed their LOS modifications using MALDI-TOF/MS. The results revealed that colistin and polymyxin B resistance was entirely lost in strains lacking pEtN modification-related genes (*pmrC* and *eptA*). In contrast, resistance was not diminished in strains lacking the GalN modification-related gene (*naxD*; Fig. 6A; Fig. S6B). The peak of pEtN modification of lipid A (*m/z* 2033), observed for strain CM012S, was absent for strains Δ*pmrA*-CM012S, Δ*pmrC*Δ*eptA*-CM012S, and Δ*pmrC*Δ*eptA*Δ*naxD*-CM012S. However, this peak was present for strain Δ*naxD*-CM012S (Fig. 6B; Fig. S5), suggesting that lipid A modification of pEtN, and not that of GalN, plays a significant role in colistin/polymyxin B resistance.

There were two genes associated with pEtN modification: *pmrC* and *eptA*, each with the solely disrupted strains Δ*pmrC*-CM012S and Δ*eptA*-CM012S showing a pEtN modification peak (Fig. 6B). This suggests that both genes are involved in pEtN modification of LOS.

DISCUSSION

In this study, we aimed to elucidate the PmrAB regulon in *A. baumannii*. The analyses identified 18 upregulated genes (Fig. 1) that encode LOS modification and polysaccharide poly-β-1,6-N-acetyl-D-glucosamine-related enzymes. Strains with disrupted LOS modification genes were created and analyzed in this study, but there is a possibility that the extracellular polysaccharide synthase genes also change the bacterial surface layer (43). These findings align with those of previous studies that used colistin-resistant clinical isolates from diverse genetic backgrounds and suggest that the regulons identified here are broadly represented across *A. baumannii* strains (31, 32). Furthermore, KAMO5_07940, which encodes an NRPS, was upregulated in PmrAB-activated mutants. Although the crystal structure of this protein has been determined, its function remains unknown (44). NRPSs typically comprise an operon and synthesize a single compound via multiple NRPSs (45). However, the locus of KAMO5_07940 does not comprise an operon, which suggests that it may function independently. Future studies should

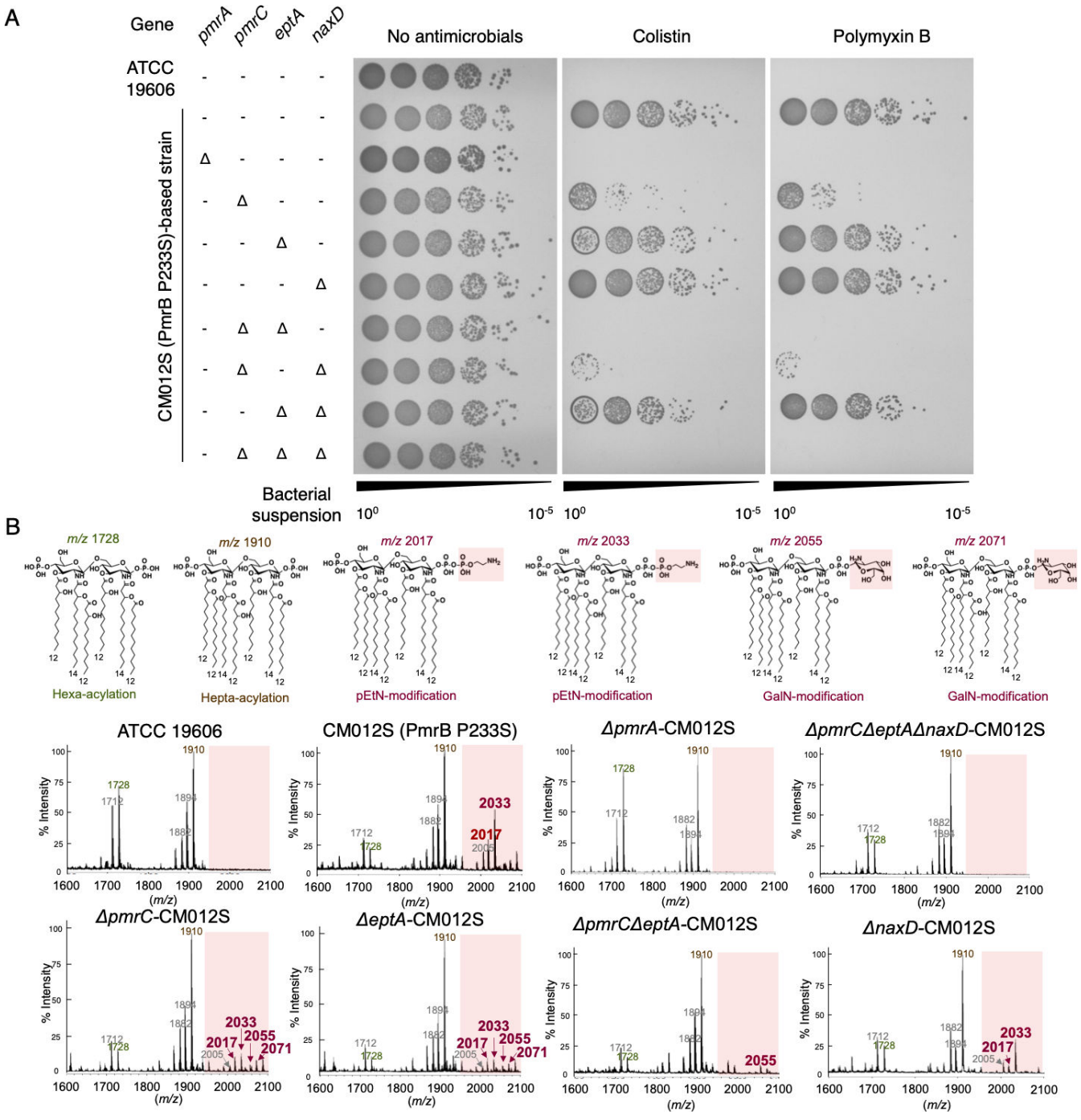

FIG 6 Effect of phosphoethanolamine and galactosamine modifications on colistin and polymyxin B resistance in *A. baumannii*. (A) Resistance to colistin and polymyxin B was evaluated for ATCC 19606 and CM012S (PmrB P233S-activating mutant strain) strains following the disruption of various LOS modification genes (*pmrC*, *eptA*, *naxD*), and in CM012S strain following the disruption of *pmrA*. The strains were cultured to reach a steady state, washed with PBS, and prepared in PBS to achieve an OD_{600} of 0.2. Subsequently, a 10-fold serial dilution (from 10^{-1} to 10^{-5}) of the bacterial suspension was prepared. This diluted suspension was then plated onto LB agar medium containing 10 µg/mL colistin and 10 µg/mL polymyxin B, which was incubated for 24 h at 37°C. Experiments were performed independently in triplicate, and representative agar plates are shown. (B) Lipid A was extracted from each strain, and MALDI-TOF/MS was used to analyze its structure. The predicted structures of lipid A and their corresponding peak mass-to-charge ratios are displayed at the top.

elucidate the biological significance of this NRPS, which is upregulated by PmrAB. Additionally, a DNA consensus sequence was found upstream of these upregulated genes, excluding those forming an operon. This sequence correlates with the

DNA-binding sequence predicted based on the PmrA protein structure (46), and PmrA is thought to bind to this motif sequence. Conversely, 12 genes were observed to be downregulated upon PmrAB activation (Fig. S7). Notably, this downregulation was not evident for the ATCC BAA-1605 strain (Fig. S8), indicating that the genetic background of individual strains influences the expression of these genes. The downregulated genes in the ATCC 19606 strain are predominantly involved in regulating intracellular iron concentrations. In contrast, the ATCC BAA-1605 strain exhibited decreased expression for a range of pili-related genes, suggesting that genes that are downregulated vary from strain to strain. Therefore, it cannot be discounted that genes downregulated by PmrAB activation may also play roles in modulating colistin resistance and virulence in *A. baumannii* (47, 48).

In this study, we found that the response of PmrB to iron ions is species dependent. Although *Salmonella* PmrB selectively recognizes Fe^{3+} (27), PmrB of *A. baumannii* is activated by Fe^{3+} under low pH conditions but not by Fe^{3+} alone (28). This suggests that because Fe^{3+} efficiently reduces to Fe^{2+} under acidic solutions, it is the reduced Fe^{2+} that activates PmrB. Unlike *Salmonella* PmrB, which does not recognize Zn^{2+}, *E. coli* PmrB does, and *A. baumannii* PmrB recognizes Zn^{2+} as well (27, 41). We identified regions in PmrB motif sequences essential for responsiveness to metal ions and pH. The results revealed the importance of the *A. baumannii* PmrB-specific ExxxE sequence, in addition to the previously considered ExxE motif, for eliciting responses to pH and Zn^{2+}. In future studies, it remains to be elucidated in detail whether these differences in metal selectivity are due to differences in amino acid sequences in and around the motif sequence or in the number of amino acid residues in the periplasmic region.

We found that PmrAB protects against excess Al^{3+} by changing the LOS in response to Al^{3+}, which is widely distributed in the environment and is mainly found in soil and rivers after acid rain (49). PmrAB senses excess Al^{3+} in the environment and upregulates the expression of the regulon's pEtN modification genes. This modification of LOS counteracts the negative charge on the bacterial surface and suppresses the effects of cations like Al^{3+} and colistin. Metal ion-induced PmrAB activation further induces LPS modification in *Salmonella* spp. (27). Although both pEtN and 4-amino-4-deoxy-L-arabinose (L-Ara4N) glycosylation modifications of LPS have been reported for *Salmonella* spp. and *E. coli*, L-Ara4N modification is more crucial for polymyxin B resistance than pEtN modification (24, 50). *A. baumannii* does not possess the L-Ara4N modification genes (such as aminoarabinose transferase *arnT* gene); however, it possesses a similar glycosylation (GalN) modification gene—the *naxD*. NaxD is a deacetylase and is unlikely to perform GalN modification alone. Activated PmrAB also enhanced the expression of three genes (KAMO5_08210, KAMO5_08220, and KAMO5_08230) downstream of the *naxD* gene (KAMO5_08240), named the *naxD* operon, suggesting that these genes are responsible for GalN modification in a coordinated manner. The mRNA levels of the *naxD* operon increased during Al^{3+} stimulation (Fig. S9A). We thus concluded that, for colistin and polymyxin B resistance and the avoidance of Al^{3+} toxicity in *A. baumannii*, pEtN modification is more critical than GalN modification by the *naxD* operon. These differences could be attributed to structural differences in the LPS of *Salmonella* spp. and *E. coli* and that of *A. baumannii*, such as the presence or absence of the O antigen (51–53), or differences in the number of acyl groups (12, 54, 55). A recent study on lipid A structure analysis of polymyxin B-resistant *A. baumannii* clinical strains reported the presence of pEtN modification but not that of GalN modification (56), which aligns with our results on PmrAB mutant strains (Fig. 6; Fig. S7). Although a small GalN modification peak (*m/z* 2071 and 2055) was observed for the pEtN modification gene disruption strains (Δ*pmrC*-CM012S, Δ*eptA*-CM012S, Δ*pmrC*Δ*eptA*-CM012S; Fig. 6B), the involvement of the *naxD* gene in LOS modification cannot be completely excluded. Because a GalN modification peak was observed in a strain in which the pEtN modification genes were disrupted, pEtN and GalN modification may competitively compete for the phosphate group, which is the modification site of lipid A. Therefore, the *naxD* operon, regulated by PmrAB, may have roles in LOS modification and other functions.

The *eptA* gene is activated following insertion into its promoter region by the insertion sequence IS*Aba1*, a process associated with the acquisition of resistance to colistin and polymyxin B (57, 58). The expression of *eptA* may be regulated by PmrAB, but this was not experimentally demonstrated. Increased *eptA* expression in PmrAB-activating mutants and Al^{3+}-stimulated WT strain (Fig. 1; Fig. S9B) and the presence of a putative PmrA-binding sequence in the *eptA* promoter region was confirmed (Fig. 2B). Moreover, a pEtN modification peak of lipid A was observed when only Δ*pmrC* or Δ*eptA* was disrupted, but this modification peak disappeared in the strain with double disruption of Δ*pmrC*Δ*eptA* (Fig. 6B). This suggests that both *pmrC* and *eptA* are genes involved in the pEtN modification of lipid A. However, based on differences in the growth of *pmrC* and *eptA* mutants in colistin and polymyxin B agar, *pmrC* may contribute more to resistance to those antimicrobials (Fig. 6A). The reason may be due to differences in the expression levels of both genes, whereby *pmrC* is more highly expressed in PmrAB-active mutants than *eptA* (Fig. 1C). In the *A. baumannii* reference strain ATCC 19606, both the *pmrC* and *eptA* genes are present on the chromosome, but ATCC BAA-1605 does not have an *eptA* gene. Conversely, some clinical isolates possess multiple *eptA* genes (57, 58). The detailed relationship between *pmrC* and *eptA* and the impact of *eptA* copy number on colistin resistance are topics for future research.

In this study, we comprehensively analyzed the PmrAB regulon and its responses in *A. baumannii* (Fig. 7). We revealed that PmrAB, previously considered to be solely involved in the drug resistance mechanism, also exhibits biological functions in response to various environmental factors, such as metal ions, in addition to colistin resistance. The biological functions of PmrAB, as revealed in this study, are essential for understanding drug resistance, environmental adaptation, and infection in bacteria, which contributes to a more comprehensive understanding of *A. baumannii*.

MATERIALS AND METHODS

Bacterial strains and growth conditions

The type strain of *A. baumannii* ATCC 19606 and drug-resistant clinical isolate ATCC BAA-1605 were acquired from ATCC (Manassas, VA, USA). The bacteria were incubated in LB broth (BD Biosciences, San Diego, CA, USA) at 37°C for 18 h with shaking at 135 rpm. Colistin-resistant strains of *A. baumannii* were established in a previous study (33).

Plasmid construction

The pSBKT3 (kanamycin resistance gene; counter-selection gene: *sacB*) and pSBKT5v2 (kanamycin resistance gene; counter-selection gene: *tdk*) plasmids were used for homologous recombination. The reporter assay also used the pProZ-Pnrps plasmid (kanamycin resistance gene; reporter marker: lacZ). Each target gene of *A. baumannii* was subcloned into these plasmids using In-Fusion cloning (Takara Bio, Shiga, Japan). The primers used for this process are listed in Table S1 and S2. These plasmids were then transformed either into *A. baumannii* by electroporation or into S17-1 λpir by heat shock.

Generation of *A. baumannii* mutant strains by two-step homologous recombination

Genetic mutants were created using a two-step homologous recombination method. S17-1 λpir harboring plasmids pSBKT3 or pSBKT5v2 and *A. baumannii* were conjugated on LB agar for 3–6 h. Subsequently, the bacteria were harvested and selected for *A. baumannii* on M9 agar (Sigma-Aldrich, St. Louis, MO, USA) containing 0.3% citric acid as the carbon source and 50 µg/mL kanamycin (both from Fujifilm Wako Pure Chemical, Osaka, Japan). The colonies formed were collected by blue-white selection on X-gal agar (Shimadzu Diagnostics, Tokyo, Japan) containing 50 µg/mL kanamycin. For pSBKT3, the counter-selection was conducted by growing the recombinant *A. baumannii* on LB agar containing 20% sucrose (Fujifilm Wako Pure Chemical) and incubating for 18–20 h at

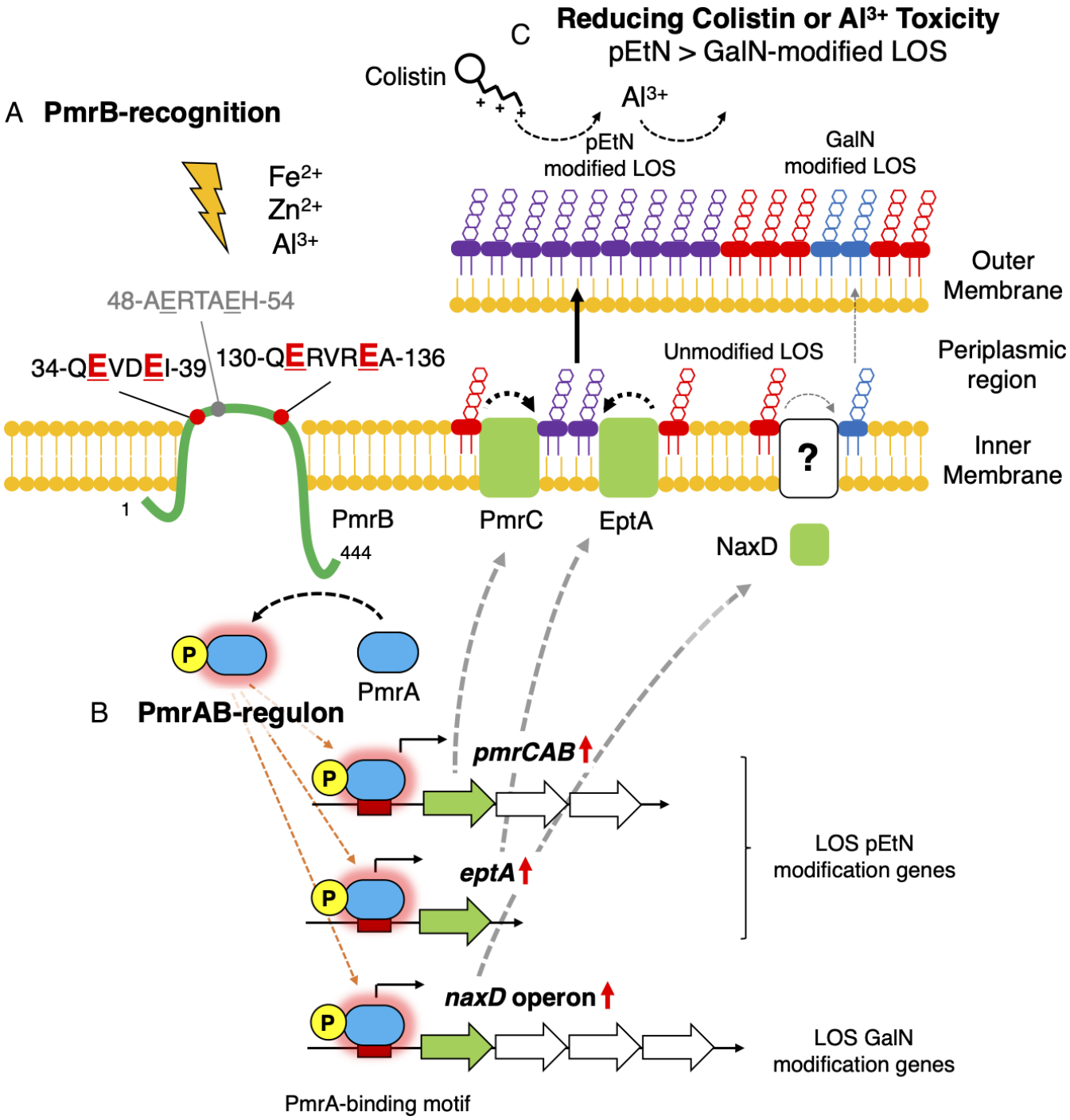

FIG 7 Schematic diagram of phosphoethanolamine modification of lipopolysaccharide by PmrAB of *A. baumannii* in response to metal ions. (A) PmrAB of *A. baumannii* is a two-component system that governs responses to Fe^{2+}, Zn^{2+}, and Al^{3+}. The 35-ExxE and 131-ExxxE motif sequences located in the periplasmic region of PmrB, a sensor kinase, are critical to these responses. (B) Among the genes activated by PmrAB are those responsible for LOS modification, which include *pmrC* and *eptA* genes for pEtN modification and *naxD* operon for GalN modification. (C) The pEtN modification of LOS is crucial for reducing Al^{3+} toxicity and for resistance to colistin. In *A. baumannii*, PmrAB is activated in response to metal ions, which leads to an upregulation of pEtN modification genes. This upregulation contributes to colistin and Al^{3+} toxicity avoidance by facilitating the modification of LOS with pEtN.

37°C. Strains with pSBKT5v2 were counter-selected after induction by isopropyl β-D-1-thiogalactopyranoside (IPTG) for *tdk*. For strains that completed the first recombination using pSBKT5v2, *A. baumannii* was inoculated into LB broth containing 50 µg/mL kanamycin and was cultured at 37°C for 18–20 h with shaking at 135 rpm. This bacterial

culture was further cultivated in LB broth without antibiotics until the OD_{600} reached 0.5–0.8, at which point IPTG (Fujifilm Wako Pure Chemical) was added to a final concentration of 1 mM and was cultured for 3 h. Counter-selection was then performed using LB agar coated with 100 µL of 200 µg/mL azidothymidine (Tokyo Chemical Industry, Tokyo, Japan).

Whole-genome sequencing

Genomic DNA was extracted from bacteria incubated for 18 h at 37°C using the DNeasy Blood and Tissue Kit (Qiagen, Hilden, Germany) and Genomic-tip (Qiagen). Sequencing libraries were prepared by Azenta (Chelmsford, MA, USA) or Genome-Lead (Kagawa, Japan). The library was prepared using the NEBNext Ultra II FS DNA Library Preparation Kit for Illumina (New England BioLabs, Ipswich, MA, USA) or Illumina DNA Prep Tagmentation (Illumina, San Diego, CA, USA), following the manufacturer's instructions. Sequencing was conducted on an Illumina HiSeq X Ten or NovaSeq 6000 sequencer (Illumina) using the 2 × 150 bp sequencing format.

To obtain the complete reference genome sequence of ATCC BAA-1605, long-read sequencing analysis was conducted using Oxford Nanopore sequencing technology (Oxford Nanopore Technologies, Oxford, UK). After preparing barcoded libraries with the Rapid Barcoding Kit (Oxford Nanopore Technologies), sequence analysis was performed on the MinION Mk1B (Oxford Nanopore Technologies), with base calls generated using Guppy v6.4.6 (Oxford Nanopore Technologies) (59). Whole-genome sequences were assembled using Unicycler v0.5.0 (60). Open reading frames and RNA regions were annotated using Prokka v1.14.5 (61) with GCA_025995075.1 as the primary database.

For mutation analysis, fastq data were quality checked and trimmed using TrimGalore v0.6.10. The sequences were then annotated using the ATCC 19606 genome sequence (GenBank accession number: AP025740.1) and the ATCC BAA-1605 genome sequence (GenBank accession number: AP029033.1-AP029034.1) as references. Mutation analysis was performed using breseq v0.36.0 (62).

RNA sequencing

Total RNA from *A. baumannii* showing logarithmic growth was extracted using NucleoSpin RNA (Macherey-Nagel) according to the manufacturer's instructions (three biological replicates). The library for sequencing was prepared by the Genome-Lead using the MGIEasy Adapters-96 kit (MGI, Shenzhen, China), and 2 × 150 bp sequences were obtained using the DNBSEQ T7 sequencer (MGI).

Fastq files were quality assessed, and adapters were removed using TrimGalore v0.6.10. These trimmed reads were then mapped to the reference genomes of *A. baumannii* ATCC 19606 (GenBank accession number: AP025740.1) and ATCC BAA-1605 (GenBank accession number: AP029033.1-AP029034.1) using HISAT2 v2.2.1 (63). The mapping data were sorted with SAMtools v1.17 (64), and aligned reads in the open reading frames of the genome were counted using the Subread package featureCounts v2.0.1 (65). Differences in gene expression were analyzed using the DESeq2 v1.34.0 package (Bioconductor) (66). Genes with an adjusted P value < 0.05 and $|\log_2$ (fold change)$| \geq 2$ were considered differentially expressed genes.

Venn diagrams, heatmaps, volcano plots, and genome distribution plots were generated using Python modules venn, venn2, Biopython, and seaborn, and by calculating and drawing custom Venn diagrams (https://bioinformatics.psb.ugent.be/webtools/Venn/). Homologs of ATCC 19606 and ATCC BAA-1605 were defined in BLASTp with an e-value ≤ 1e-10 and % identity ≥ 90%.

Real-time and endpoint PCR

Total RNA from the indicated *A. baumannii* strains was extracted using TRI-Reagent (Molecular Research Center, Cincinnati, OH, USA). The total RNA was treated with DNase I (Nippon Gene, Tokyo, Japan) to remove genomic DNA; reverse transcription from RNA

to cDNA was performed using the PrimeScript RT Reagent Kit (Takara Bio); and real-time PCR was performed using SYBR Green ExTaq II (Takara Bio) with primers listed in Table S3. The amplification and detection of PCR products were carried out on a Thermal Cycler Dice Real Time System III (Takara Bio). Endpoint PCR was performed using GoTaq Master Mix (Table S4; Promega, Madison, WI, USA) in constant cycles.

Reporter assay

Strains harboring the reporter plasmid were incubated in LB broth containing 50 µg/mL kanamycin for 18 h at 37°C with shaking at 135 rpm. The culture was then diluted 100-fold in LB broth containing 50 µg/mL kanamycin and was incubated at 37°C with shaking at 135 rpm to reach an OD_{600} of 0.1–0.5. Subsequently, the strains were exposed to specific stresses [500 µM NaCl, KCl, $MgCl_2$, $CaCl_2$, $FeSO_4$, $FeCl_3$, $ZnSO_4$, $AlCl_3$, $NiSO_4$, $Co(NO_3)_2$, $MnCl_2$, or $CuSO_4$ (Fujifilm Wako Pure Chemical), or pH 5.8] for 60 min at 37°C. The bacteria were then lysed using toluene (Fujifilm Wako Pure Chemical; 20-µL toluene for 700 µL of suspension), following which the toluene was evaporated by incubation at 37°C for 60 min. The lysate was mixed with Z buffer (60 mM Na_2HPO_4, 40 mM NaH_2PO_4, 10 mM KCl, 1 mM $MgSO_4$, and 50 mM β-mercaptoethanol; all from Fujifilm Wako Pure Chemical). The lysate was then mixed with 20 µL of *o*-nitrophenyl-β-D-galactopyranoside solution (4 mg/mL *o*-nitrophenyl-β-galactoside [Fujifilm Wako Pure Chemical] in 100-mM sodium phosphate buffer, pH 7.0), following which 100 µL of the solution was added to a 96-well plate for 15–60 min at 28°C. The reaction was stopped by adding 50 µL of 1 M Na_2CO_3 (Fujifilm Wako Pure Chemical). Absorbance A_{420} and A_{600} were measured using Varioskan (Thermo Fisher Scientific, Waltham, MA, USA), and β-galactosidase activity was calculated in Miller Units and then expressed as a relative value. The reaction equation used is as follows: Miller Units = $1{,}000 \times [A_{420}(x\ min) - A_{420}(0\ min)] / [reaction\ time\ (x\ min) \times reaction\ vol\ (mL) \times A_{600}]$.

Short-term polymyxin bactericidal assay

The resistance of bacteria to short-term exposure to polymyxins was evaluated by exposing the bacteria to an antimicrobial agent for 2 h and subsequently detecting the bacteria that survived this exposure. Induction with Al^{3+} was performed by shaking at 135 rpm for 2 h, with or without the addition of 500 µM $AlCl_3$. The bacteria were washed twice with phosphate-buffered saline (PBS) and were adjusted to an OD_{600} of 0.2. This solution was then incubated with 10 µg/mL colistin and 7 µg/mL polymyxin B for 2 h. After sterilization, a 10-fold dilution series of the bacterial solution was prepared, and 10 µL of each dilution was plated onto LB agar plates without any antimicrobial agents. The plates were incubated for 18–20 h at 37°C. The number of colonies on the plates was counted to evaluate the effectiveness of the sterilization process.

Long-term polymyxin bactericidal assay

The bacterial solution was incubated for 18 h in LB broth at 37°C with shaking at 135 rpm, washed with PBS, and prepared in PBS to achieve an OD_{600} of 0.2. A 10-fold dilution series of this solution was prepared, and 10 µL of each dilution was plated onto LB agar containing 10 µg/mL colistin and 10 µg/mL polymyxin B. These plates were incubated for 18–20 h at 37°C. The effectiveness of the bactericidal treatment was assessed by counting the number of colonies.

Metal-induced bacterial growth inhibition assay

The bacteria were initially incubated in LB broth for 18 h at 37°C with shaking at 135 rpm. Subsequently, these were prepared in LB broth containing varying concentrations of $AlCl_3$ (0, 0.5, 1, 1.5, 2, 2.5, or 3 mM) to achieve an OD_{600} of 0.001. This bacterial suspension was incubated in 96-well plates for 24 h at 37°C. The absorbance at A_{600} was measured using Varioskan, and the relative values of A_{600} in the presence and absence of

metal ions were calculated. This process was conducted to evaluate the bacteria's growth and growth inhibition capabilities.

Analysis of lipid A by MALDI-TOF/MS

Lipid A of LOS was extracted using the ammonium hydroxide/isobutyric acid method (67), with some modifications. Briefly, lyophilized bacteria from 3 or 10 mL of culture medium that had been incubated for 18 h at 37°C with shaking were resuspended in 400 µL of isobutyric acid/1 M ammonium hydroxide (5:3, vol/vol; Fujifilm Wako Pure Chemical) and were heated for 2 h at 100°C. After cooling, the samples were centrifuged at 2,000 × *g* for 15 min at 4°C. An equal volume of ultrapure water was added to the supernatant, which was then lyophilized. The residue was washed twice with 1 mL of methanol (Fujifilm Wako Pure Chemical) and was centrifuged at 2,000 × *g* for 15 min at 4°C. The insoluble lipid A was solubilized in 1 mL of chloroform/methanol/water (3:1.5:0.25, vol/vol/vol; Fujifilm Wako Pure Chemical) and was centrifuged at 10,000 × *g* for 3 min at 4°C, following which the supernatant was collected. The collected supernatant was mixed with 1 mL of water and was centrifuged at 400 × *g* for 30 s at 4°C, following which the lipid A fraction (lower layer) was collected. The lipid A fraction from which the solvent was removed by flushing with N_2 gas was dissolved in 100 µL of chloroform/methanol (2:1, vol/vol) and was mixed with an equal volume of a matrix (10 mg/mL 2,5-dihydroxybenzoic acid in water/methanol [7:3, vol/vol] containing 0.1% [wt/vol] trifluoroacetic acid) on a target plate. MALDI-TOF/MS analysis was performed using an UltrafleXtreme-DHS2 TOF/TOF (Bruker Daltonics, Billerica, MA, USA) instrument in negative-reflective mode. The chemical modifications of lipid A were evaluated based on the obtained MALDI-TOF mass spectra.

Determination of colistin MICs

The MICs for colistin were determined using the microdilution method in LB broth (BD Biosciences) as previously described (68). Briefly, the bacterial culture was adjusted to an OD_{600} of 0.001 using freshly prepared LB broth, with or without the addition of 500 µM Al^{3+} from overnight cultures. The MICs for colistin were monitored using a twofold dilution series starting at 256 µg/mL.

Statistical analysis

Statistical analysis was performed using R software (R Foundation for Statistical Computing, Vienna, Austria). Data are expressed as means ± standard deviation and were compared using unpaired *t*-test or the one-way analysis of variance and Dunnett's test or Tukey's test. Differences with *P* values of < 0.05 were considered statistically significant.

ACKNOWLEDGMENTS

We thank Atsushi Yokotani (Kyoto Pharmaceutical University) and Tohru Miyoshi-Akiyama (National Center for Global Health and Medicine) for their helpful discussions regarding this study. We also thank Tomoka Nakamura, Tomoko Okada, Sayaka Nagamine, Yurika Hishikawa, Mitsuki Okuda (Kyoto Pharmaceutical University), and Yu Sakurai (National Center for Global Health and Medicine) for their technical assistance. We thank the Open Facility, Global Facility Center, Creative Research Institution, Hokkaido University for allowing us to conduct the lipid A analysis using UltrafleXtreme-DHS2 TOF/TOF (Bruker Daltonics). We thank Editage for English language editing.

This work was supported in part by the Ministry of Education, Culture, Sports, Science, and Technology of Japan, the Science Research Promotion Fund to G.K. (17K16230, 20K17475), the Kanehara Ichiro Memorial Foundation to G.K., the Morinomiyako Medical Research Foundation to G.K., the Kyoto Pharmaceutical University Fund for the Promotion of Scientific Research to G.K., and a grant from Agency for Medical Research and

Development (AMED) to K.Y. (22fk0108611h0902). The funders had no role in the study design, data collection, interpretation, or the decision to submit the work for publication.

Methodology: N.Y. and G.K.; formal analysis: N.Y. and G.K.; investigation: N.Y., G.K., T.S., D.Y., M.M., R.Y., N.K., R.K., and N.T.; writing – original draft: N.Y. and G.K.; supervision: Y.M., M.F., S.Y., and K.Y.

The authors declare no competing financial interests.

AUTHOR AFFILIATIONS

[1]Laboratory of Microbiology and Infection Control, Kyoto Pharmaceutical University, Kyoto, Japan
[2]Laboratory of Cell Biology, Kyoto Pharmaceutical University, Kyoto, Japan
[3]Department of Infection Control Science, Meiji Pharmaceutical University, Tokyo, Japan
[4]Department of Microbiology, Sapporo Medical University School of Medicine, Hokkaido, Japan
[5]Pathogenic Microbe Laboratory, Research Institute, National Center for Global Health and Medicine, Tokyo, Japan

AUTHOR ORCIDs

Go Kamoshida http://orcid.org/0000-0001-6300-0911
Masahiro Fujimuro https://orcid.org/0000-0002-5165-0789

FUNDING

Funder	Grant(s)	Author(s)
MEXT | Japan Society for the Promotion of Science (JSPS)	17K16230, 20K17475	Go Kamoshida
Ichiro Kanehara Foundation for the Promotion of Medical Sciences and Medical Care (Ichiro Kanehara Foundation)		Go Kamoshida
Morinomiyako Medical Research		Go Kamoshida
Kyoto Pharmaceutical University (KPU)		Go Kamoshida
Japan Agency for Medical Research and Development (AMED)	22fk0108611h0902	Kinnosuke Yahiro

DATA AVAILABILITY

The original data sets are available in publicly accessible repositories. The genome sequencing data of representative *A. baumannii* isolates from this study have been deposited in the DNA Data Bank of Japan under BioProject accession numbers PRJDB12922 and PRJDB16715. The RNA sequencing data of *A. baumannii* isolates were also registered (BioProject accession number PRJDB16717). Additionally, the GenBank file for the whole-genome sequence data of ATCC BAA-1605 (BioProject accession number PRJDB16714) has been registered with the DNA Data Bank of Japan.

ADDITIONAL FILES

The following material is available online.

Supplemental Material

Supplemental figures (JB00435-23-S0001.docx). Figures S1 to S9.
Supplemental tables (JB00435-23-S0002.docx). Tables S1 to S4.

REFERENCES

1. Mea HJ, Yong PVC, Wong EH. 2021. An overview of *Acinetobacter baumannii* pathogenesis: motility, adherence and biofilm formation. Microbiol Res 247:126722. https://doi.org/10.1016/j.micres.2021.126722
2. Bassetti M, Vena A, Battaglini D, Pelosi P, Giacobbe DR. 2020. The role of new antimicrobials for Gram-negative infections in daily clinical practice. Curr Opin Infect Dis 33:495–500. https://doi.org/10.1097/QCO.0000000000000686
3. Gonzalez-Villoria AM, Valverde-Garduno V. 2016. Antibiotic-resistant *Acinetobacter baumannii* increasing success remains a challenge as a nosocomial pathogen. J Pathog 2016:7318075. https://doi.org/10.1155/2016/7318075
4. Bassetti M, Righi E. 2015. New antibiotics and antimicrobial combination therapy for the treatment of gram-negative bacterial infections. Curr Opin Crit Care 21:402–411. https://doi.org/10.1097/MCC.0000000000000235
5. Giamarellou H, Antoniadou A, Kanellakopoulou K. 2008. *Acinetobacter baumannii*: a universal threat to public health? Int J Antimicrob Agents 32:106–119. https://doi.org/10.1016/j.ijantimicag.2008.02.013
6. Dijkshoorn L, Nemec A, Seifert H. 2007. An increasing threat in hospitals: multidrug-resistant *Acinetobacter baumannii*. Nat Rev Microbiol 5:939–951. https://doi.org/10.1038/nrmicro1789
7. Doi Y, Husain S, Potoski BA, McCurry KR, Paterson DL. 2009. Extensively drug-resistant *Acinetobacter baumannii*. Emerg Infect Dis 15:980–982. https://doi.org/10.3201/eid1506.081006
8. Papp-Wallace KM, Endimiani A, Taracila MA, Bonomo RA. 2011. Carbapenems: past, present, and future. Antimicrob Agents Chemother 55:4943–4960. https://doi.org/10.1128/AAC.00296-11
9. Poirel L, Nordmann P. 2006. Carbapenem resistance in *Acinetobacter baumannii*: mechanisms and epidemiology. Clin Microbiol Infect 12:826–836. https://doi.org/10.1111/j.1469-0691.2006.01456.x
10. Nguyen M, Joshi SG. 2021. Carbapenem resistance in *Acinetobacter baumannii*, and their importance in hospital-acquired infections: a scientific review. J Appl Microbiol 131:2715–2738. https://doi.org/10.1111/jam.15130
11. Almutairi MM. 2022. Synergistic activities of colistin combined with other antimicrobial agents against colistin-resistant *Acinetobacter baumannii* clinical isolates. PLoS One 17:e0270908. https://doi.org/10.1371/journal.pone.0270908
12. Powers MJ, Trent MS. 2018. Expanding the paradigm for the outer membrane: *Acinetobacter baumannii* in the absence of endotoxin. Mol Microbiol 107:47–56. https://doi.org/10.1111/mmi.13872
13. Cafiso V, Stracquadanio S, Lo Verde F, Gabriele G, Mezzatesta ML, Caio C, Pigola G, Ferro A, Stefani S. 2018. Colistin resistant *A. baumannii*: genomic and transcriptomic traits acquired under colistin therapy. Front Microbiol 9:3195. https://doi.org/10.3389/fmicb.2018.03195
14. Qureshi ZA, Hittle LE, O'Hara JA, Rivera JI, Syed A, Shields RK, Pasculle AW, Ernst RK, Doi Y. 2015. Colistin-resistant *Acinetobacter baumannii*: beyond carbapenem resistance. Clin Infect Dis 60:1295–1303. https://doi.org/10.1093/cid/civ048
15. Chen Z, Chen Y, Fang Y, Wang X, Chen Y, Qi Q, Huang F, Xiao X. 2015. Meta-analysis of colistin for the treatment of *Acinetobacter baumannii* infection. Sci Rep 5:17091. https://doi.org/10.1038/srep17091
16. Karakonstantis S. 2021. A systematic review of implications, mechanisms, and stability of *in vivo* emergent resistance to colistin and tigecycline in *Acinetobacter baumannii*. J Chemother 33:1–11. https://doi.org/10.1080/1120009X.2020.1794393
17. Gogry FA, Siddiqui MT, Sultan I, Haq QMR. 2021. Current update on intrinsic and acquired colistin resistance mechanisms in bacteria. Front Med (Lausanne) 8:677720. https://doi.org/10.3389/fmed.2021.677720
18. Chin CY, Gregg KA, Napier BA, Ernst RK, Weiss DS. 2015. A PmrB-regulated deacetylase required for lipid A modification and polymyxin resistance in *Acinetobacter baumannii*. Antimicrob Agents Chemother 59:7911–7914. https://doi.org/10.1128/AAC.00515-15
19. Arroyo LA, Herrera CM, Fernandez L, Hankins JV, Trent MS, Hancock REW. 2011. The pmrCAB operon mediates polymyxin resistance in *Acinetobacter baumannii* ATCC 17978 and clinical isolates through phosphoethanolamine modification of lipid A. Antimicrob Agents Chemother 55:3743–3751. https://doi.org/10.1128/AAC.00256-11
20. Beceiro A, Llobet E, Aranda J, Bengoechea JA, Doumith M, Hornsey M, Dhanji H, Chart H, Bou G, Livermore DM, Woodford N. 2011. Phosphoethanolamine modification of lipid A in colistin-resistant variants of *Acinetobacter baumannii* mediated by the pmrAB two-component regulatory system. Antimicrob Agents Chemother 55:3370–3379. https://doi.org/10.1128/AAC.00079-11
21. Chen HD, Groisman EA. 2013. The biology of the PmrA/PmrB two-component system: the major regulator of lipopolysaccharide modifications. Annu Rev Microbiol 67:83–112. https://doi.org/10.1146/annurev-micro-092412-155751
22. Gunn JS. 2008. The *Salmonella* PmrAB regulon: lipopolysaccharide modifications, antimicrobial peptide resistance and more. Trends Microbiol 16:284–290. https://doi.org/10.1016/j.tim.2008.03.007
23. Kato A, Higashino N, Utsumi R. 2017. Fe(3+)-dependent epistasis between the CpxR-activated loci and the PmrA-activated LPS modification loci in *Salmonella enterica*. J Gen Appl Microbiol 62:286–296. https://doi.org/10.2323/jgam.2016.05.005
24. Kato A, Chen HD, Latifi T, Groisman EA. 2012. Reciprocal control between a bacterium's regulatory system and the modification status of its lipopolysaccharide. Mol Cell 47:897–908. https://doi.org/10.1016/j.molcel.2012.07.017
25. Perez JC, Groisman EA. 2007. Acid pH activation of the PmrA/PmrB two-component regulatory system of *Salmonella enterica*. Mol Microbiol 63:283–293. https://doi.org/10.1111/j.1365-2958.2006.05512.x
26. Nishino K, Hsu F-F, Turk J, Cromie MJ, Wösten M, Groisman EA. 2006. Identification of the lipopolysaccharide modifications controlled by the *Salmonella* PmrA/PmrB system mediating resistance to Fe(III) and Al(III). Mol Microbiol 61:645–654. https://doi.org/10.1111/j.1365-2958.2006.05273.x
27. Wösten MM, Kox LF, Chamnongpol S, Soncini FC, Groisman EA. 2000. A signal transduction system that responds to extracellular iron. Cell 103:113–125. https://doi.org/10.1016/s0092-8674(00)00092-1
28. Ko SY, Kim N, Park SY, Kim SY, Shin M, Lee JC. 2023. *Acinetobacter baumannii* under acidic conditions induces colistin resistance through PmrAB activation and lipid A modification. Antibiotics (Basel) 12:813. https://doi.org/10.3390/antibiotics12050813
29. Adams MD, Nickel GC, Bajaksouzian S, Lavender H, Murthy AR, Jacobs MR, Bonomo RA. 2009. Resistance to colistin in *Acinetobacter baumannii* associated with mutations in the PmrAB two-component system. Antimicrob Agents Chemother 53:3628–3634. https://doi.org/10.1128/AAC.00284-09
30. De Silva PM, Kumar A. 2019. Signal transduction proteins in *Acinetobacter baumannii*: role in antibiotic resistance, virulence, and potential as drug targets. Front Microbiol 10:49. https://doi.org/10.3389/fmicb.2019.00049
31. Wright MS, Jacobs MR, Bonomo RA, Adams MD. 2017. Transcriptome remodeling of *Acinetobacter baumannii* during infection and treatment. mBio 8:e02193-16. https://doi.org/10.1128/mBio.02193-16
32. Park YK, Lee JY, Ko KS. 2015. Transcriptomic analysis of colistin-susceptible and colistin-resistant isolates identifies genes associated with colistin resistance in *Acinetobacter baumannii*. Clin Microbiol Infect 21:765. https://doi.org/10.1016/j.cmi.2015.04.009
33. Kamoshida G, Yamada N, Nakamura T, Yamaguchi D, Kai D, Yamashita M, Hayashi C, Kanda N, Sakaguchi M, Morimoto H, Sawada T, Okada T, Kaya Y, Takemoto N, Yahiro K. 2022. Preferential selection of low-frequency, lipopolysaccharide-modified, colistin-resistant mutants with a combination of antimicrobials in *Acinetobacter baumannii*. Microbiol Spectr 10:e0192822. https://doi.org/10.1128/spectrum.01928-22
34. Charretier Y, Diene SM, Baud D, Chatellier S, Santiago-Allexant E, van Belkum A, Guigon G, Schrenzel J. 2018. Colistin heteroresistance and involvement of the PmrAB regulatory system in *Acinetobacter baumannii*. Antimicrob Agents Chemother 62:e00788-18. https://doi.org/10.1128/AAC.00788-18
35. Mustapha MM, Li B, Pacey MP, Mettus RT, McElheny CL, Marshall CW, Ernst RK, Cooper VS, Doi Y. 2018. Phylogenomics of colistin-susceptible and resistant XDR *Acinetobacter baumannii*. J Antimicrob Chemother 73:2952–2959. https://doi.org/10.1093/jac/dky290

36. Dafopoulou K, Xavier BB, Hotterbeekx A, Janssens L, Lammens C, Dé E, Goossens H, Tsakris A, Malhotra-Kumar S, Pournaras S. 2016. Colistin-resistant *Acinetobacter baumannii* clinical strains with deficient biofilm formation. Antimicrob Agents Chemother 60:1892–1895. https://doi.org/10.1128/AAC.02518-15
37. Bailey TL, Elkan C. 1994. Fitting a mixture model by expectation maximization to discover motifs in biopolymers. Proc Int Conf Intell Syst Mol Biol 2:28–36.
38. Ainsaar K, Mumm K, Ilves H, Hõrak R. 2014. The ColRS signal transduction system responds to the excess of external zinc, iron, manganese, and cadmium. BMC Microbiol 14:162. https://doi.org/10.1186/1471-2180-14-162
39. Krogh A, Larsson B, von Heijne G, Sonnhammer EL. 2001. Predicting transmembrane protein topology with a hidden Markov model: application to complete genomes. J Mol Biol 305:567–580. https://doi.org/10.1006/jmbi.2000.4315
40. Jaiswal SK, Naamala J, Dakora FD. 2018. Nature and mechanisms of aluminium toxicity, tolerance and amelioration in symbiotic legumes and rhizobia. Biol Fertil Soils 54:309–318. https://doi.org/10.1007/s00374-018-1262-0
41. Lee LJ, Barrett JA, Poole RK. 2005. Genome-wide transcriptional response of chemostat-cultured *Escherichia coli* to zinc. J Bacteriol 187:1124–1134. https://doi.org/10.1128/JB.187.3.1124-1134.2005
42. Chamnongpol S, Dodson W, Cromie MJ, Harris ZL, Groisman EA. 2002. Fe(III)-mediated cellular toxicity. Mol Microbiol 45:711–719. https://doi.org/10.1046/j.1365-2958.2002.03041.x
43. Henry R, Vithanage N, Harrison P, Seemann T, Coutts S, Moffatt JH, Nation RL, Li J, Harper M, Adler B, Boyce JD. 2012. Colistin-resistant, lipopolysaccharide-deficient *Acinetobacter baumannii* responds to lipopolysaccharide loss through increased expression of genes involved in the synthesis and transport of lipoproteins, phospholipids, and poly-beta-1,6-*N*-acetylglucosamine. Antimicrob Agents Chemother 56:59–69. https://doi.org/10.1128/AAC.05191-11
44. Drake EJ, Miller BR, Shi C, Tarrasch JT, Sundlov JA, Allen CL, Skiniotis G, Aldrich CC, Gulick AM. 2016. Structures of two distinct conformations of holo-non-ribosomal peptide synthetases. Nature 529:235–238. https://doi.org/10.1038/nature16163
45. Martínez-Núñez MA, López VELy. 2016. Nonribosomal peptides synthetases and their applications in industry. Sustain Chem Process 4. https://doi.org/10.1186/s40508-016-0057-6
46. Palethorpe S, Milton ME, Pesci EC, Cavanagh J. 2022. Structure of the *Acinetobacter baumannii* PmrA receiver domain and insights into clinical mutants affecting DNA binding and promoting colistin resistance. J Biochem 170:787–800. https://doi.org/10.1093/jb/mvab102
47. Murdoch CC, Skaar EP. 2022. Nutritional immunity: the battle for nutrient metals at the host-pathogen interface. Nat Rev Microbiol 20:657–670. https://doi.org/10.1038/s41579-022-00745-6
48. Harding CM, Hennon SW, Feldman MF. 2018. Uncovering the mechanisms of *Acinetobacter baumannii* virulence. Nat Rev Microbiol 16:91–102. https://doi.org/10.1038/nrmicro.2017.148
49. Alasfar RH, Isaifan RJ. 2021. Aluminum environmental pollution: the silent killer. Environ Sci Pollut Res Int 28:44587–44597. https://doi.org/10.1007/s11356-021-14700-0
50. Olaitan AO, Morand S, Rolain JM. 2014. Mechanisms of polymyxin resistance: acquired and intrinsic resistance in bacteria. Front Microbiol 5:643. https://doi.org/10.3389/fmicb.2014.00643
51. Roshini J, Patro LPP, Sundaresan S, Rathinavelan T. 2023. Structural diversity among *Acinetobacter baumannii* K-antigens and its implication in the *in silico* serotyping. Front Microbiol 14:1191542. https://doi.org/10.3389/fmicb.2023.1191542
52. DebRoy C, Fratamico PM, Yan X, Baranzoni G, Liu Y, Needleman DS, Tebbs R, O'Connell CD, Allred A, Swimley M, Mwangi M, Kapur V, Raygoza Garay JA, Roberts EL, Katani R. 2016. Comparison of O-antigen gene clusters of all O-serogroups of *Escherichia coli* and proposal for adopting a new nomenclature for O-typing. PLoS ONE 11:e0147434. https://doi.org/10.1371/journal.pone.0147434
53. Liu B, Knirel YA, Feng L, Perepelov AV, Senchenkova SN, Reeves PR, Wang L. 2014. Structural diversity in *Salmonella* O antigens and its genetic basis. FEMS Microbiol Rev 38:56–89. https://doi.org/10.1111/1574-6976.12034
54. Steimle A, Autenrieth IB, Frick JS. 2016. Structure and function: lipid A modifications in commensals and pathogens. Int J Med Microbiol 306:290–301. https://doi.org/10.1016/j.ijmm.2016.03.001
55. Hoare A, Bittner M, Carter J, Alvarez S, Zaldívar M, Bravo D, Valvano MA, Contreras I. 2006. The outer core lipopolysaccharide of *Salmonella enterica* serovar Typhi is required for bacterial entry into epithelial cells. Infect Immun 74:1555–1564. https://doi.org/10.1128/IAI.74.3.1555-1564.2006
56. Kim SH, Yun S, Park W. 2022. Constitutive phenotypic modification of lipid A in clinical *Acinetobacter baumannii* isolates. Microbiol Spectr 10:e0129522. https://doi.org/10.1128/spectrum.01295-22
57. Potron A, Vuillemenot J-B, Puja H, Triponney P, Bour M, Valot B, Amara M, Cavalié L, Bernard C, Parmeland L, Reibel F, Larrouy-Maumus G, Dortet L, Bonnin RA, Plésiat P. 2019. ISAba1-dependent overexpression of eptA in clinical strains of *Acinetobacter baumannii* resistant to colistin. J Antimicrob Chemother 74:2544–2550. https://doi.org/10.1093/jac/dkz241
58. Trebosc V, Gartenmann S, Tötzl M, Lucchini V, Schellhorn B, Pieren M, Lociuro S, Gitzinger M, Tigges M, Bumann D, Kemmer C. 2019. Dissecting colistin resistance mechanisms in extensively drug-resistant *Acinetobacter baumannii* clinical isolates. mBio 10:e01083-19. https://doi.org/10.1128/mBio.01083-19
59. Wick RR, Judd LM, Holt KE. 2019. Performance of neural network basecalling tools for Oxford nanopore sequencing. Genome Biol 20:129. https://doi.org/10.1186/s13059-019-1727-y
60. Wick RR, Judd LM, Gorrie CL, Holt KE. 2017. Unicycler: resolving bacterial genome assemblies from short and long sequencing reads. PLoS Comput Biol 13:e1005595. https://doi.org/10.1371/journal.pcbi.1005595
61. Seemann T. 2014. Prokka: rapid prokaryotic genome annotation. Bioinformatics 30:2068–2069. https://doi.org/10.1093/bioinformatics/btu153
62. Deatherage DE, Barrick JE. 2014. Identification of mutations in laboratory-evolved microbes from next-generation sequencing data using *breseq*. Methods Mol Biol 1151:165–188. https://doi.org/10.1007/978-1-4939-0554-6_12
63. Kim D, Langmead B, Salzberg SL. 2015. HISAT: a fast spliced aligner with low memory requirements. Nat Methods 12:357–360. https://doi.org/10.1038/nmeth.3317
64. Li H, Handsaker B, Wysoker A, Fennell T, Ruan J, Homer N, Marth G, Abecasis G, Durbin R, Genome Project Data Processing S. 2009. The sequence alignment/map format and SAMtools. Bioinformatics 25:2078–2079. https://doi.org/10.1093/bioinformatics/btp352
65. Liao Y, Smyth GK, Shi W. 2014. featureCounts: an efficient general purpose program for assigning sequence reads to genomic features. Bioinformatics 30:923–930. https://doi.org/10.1093/bioinformatics/btt656
66. Love MI, Huber W, Anders S. 2014. Moderated estimation of fold change and dispersion for RNA-seq data with DESeq2. Genome Biol 15:550. https://doi.org/10.1186/s13059-014-0550-8
67. March C, Regueiro V, Llobet E, Moranta D, Morey P, Garmendia J, Bengoechea JA. 2010. Dissection of host cell signal transduction during *Acinetobacter baumannii*-triggered inflammatory response. PLoS One 5:e10033. https://doi.org/10.1371/journal.pone.0010033
68. Kamoshida G, Akaji T, Takemoto N, Suzuki Y, Sato Y, Kai D, Hibino T, Yamaguchi D, Kikuchi-Ueda T, Nishida S, Unno Y, Tansho-Nagakawa S, Ubagai T, Miyoshi-Akiyama T, Oda M, Ono Y. 2020. Lipopolysaccharide-deficient *Acinetobacter baumannii* due to colistin resistance is killed by neutrophil-produced lysozyme. Front Microbiol 11:573. https://doi.org/10.3389/fmicb.2020.00573